PENNSTATE

College of Engineering

Department of Chemical Engineering

Designing molecular technology for the 21st century with biology and chemistry

McWhirter Graduate Research Symposium

Friday, September 16, 2022

The Graduate Hotel, State College

McWhirter Graduate Research Symposium

Friday, September 16, 2022
The Graduate Hotel, 125 S Atherton St, State College, PA 16801

8:30 AM	**Registration: 1855 Lobby**			
9:00 AM	**Session 1: Coaly Ballroom**			
9:00 AM	**Room A**		**Room B**	
9:00 AM – 9:20 AM	*Micro- and nanoengineering of biomaterials to tackle antibiotic resistance*	Shang-Lin Yeh Adv: Amir Sheikhi	*Structural inhomogeneity of cellulose assembly in plant cell wall affecting anisotropic mechanical property*	Jongcheol Lee Adv: Seong Kim
9:20 AM – 9:40 AM	*Extracellular Matrix Stiffness Regulates Histone Modifications During TGFβ1-Induced Epithelial-to-Mesenchymal Transition*	Jessica Sacco Adv: Esther Gomez	*Depth filters for removal of HCP during monoclonal antibody production*	Liang-Kai Chu Adv: Andrew Zydney
9:40 AM – 10:00 AM	*Cold Sintering–a New Approach to Reprocess Composite Electrolytes in All-Solid-State Lithium-Ion Batteries*	Yi-Chen Lan Adv: Enrique Gomez	*Investigation of the mesoscale structural assembly of cellulose microfibrils in plant cell walls using sum-frequency generation vibrational spectroscopy*	Juseok Choi Adv: Seong Kim

10:00 AM – 10:20 AM	*Understanding the effects of structure of hydrogenated diamond-like carbon on its surface oxidation and frictional behavior in O2 and H2O*	Seokhoon Jang Adv: Seong Kim	*A fundamental model to describe asymmetric ion transport in bipolar membranes*	Harrison Cassady Adv: Michael Hickner
10:20 AM	**Coffee break – 1855 Lobby**			
10:40 AM	**Session 2: Coaly Ballroom**			
10:40 AM – 11:00 AM	*Stable All-Solid-State Sodium-Sulfur Batteries Enabled by Sodium-Antimony Alloy Anode and Confined Sulfur Cathode*	Li-Ji Jhang Adv: Donghai Wang	*Rational Engineering of Explosive-sensing Soil Bacteria*	Erin Essington Adv: Howard Salis
11:00 AM – 11:20 AM	*Catalytic Co-Pyrolysis of Polyolefins and Polyethylene Terephthalate (PET) with Zeolite Catalysts*	Sean Okonsky Adv: Hilal Ezgi Toraman	*Using machine learning approaches to estimate enzyme kinetic parameters*	Veda Sheersh Boorla Adv: Costas Maranas
11:20 AM – 11:40 AM	*Designing retro-biosynthesis pathways to chemical products: Algorithmic improvements and applications*	Vikas Upadhyay Adv: Costas Maranas	*Analysis of Ribosome Regulators in the Formation and Resuscitation of Persister cells*	Joy Muthami Adv: Thomas Wood
11:40 AM – 12:00 PM	*Electricity generation from hydraulic fracturing wastewater using a reverse electrodialysis stack*	Arash Emdadi Adv: Lauren Greenlee, Bruce Logan	*Kinetic asymmetry determines the direction of enzyme chemotaxis*	Niladri Sekhar Mandal Adv: Ayusman Sen

12:00 PM	**Lunch – Provided: 1855 Lobby**	
1:00 PM	**Keynote Speaker – Dr. Colleen Severyn – Coaly Ballroom**	
2:00 PM	**Coffee break: 1855 Lobby**	
2:15 PM	**Session 3 Room A: Coaly Ballroom**	
2:15 PM – 2:35 PM	*Block copolymer templated extended surface PGM nanostructures as model electrocatalysts*	Deepra Bhattacharya Adv: Christopher Arges
2:35 PM – 2:55 PM	*Heterogeneous Catalysis with Photocatalytic Polymer Brushes on Glass Beads*	Sarah Freeburne Adv: Christian Pester
2:55 PM – 3:15 PM	*Incorporating electrode-electrolyte interfacial effects on the specific adsorption of alkali cations on late transition metal surfaces using DFT methods*	Andrew Jark-Wah Wong Adv: Michael Janik
3:15 PM – 3:35 PM	*Computational Evaluation of Selective Hydrogenation Reactions on TiO2-supported Single Atom Catalysts*	Jeremy Hu Adv: Michael Janik, Konstantinos Alexopoulos
3:35 PM – 3:55 PM	*Enhanced Electrochemical Phosphate Recovery from Wastewater: Implications of Pulsating Anode Potential*	Ruhi Sultana Adv: Lauren Greenlee, Michael Janik
4:00 PM	**Poster Session and Networking – 1855 Lobby**	

Session 1: Room A

Micro- and nanoengineering of biomaterials to tackle antibiotic resistance

Shang-Lin Yeh,[1] Amir Sheikhi[1,2]*

[1]Department of Chemical Engineering, Pennsylvania State University, University Park, PA 16802, USA

[2]Department of Biomedical Engineering, Pennsylvania State University, University Park, PA 16802, USA

*Corresponding author: Amir Sheikhi (sheikhi@psu.edu)

To combat bacterial infections in humans, antibiotics have extensively been used to save millions of lives since the 20th century. Vancomycin (VAN) and daptomycin (DAP) are important first-line antibiotics for the treatment of multidrug-resistant Gram-positive bacteria; however, the biliary excretion of intravenously administrated antibiotics in the gastrointestinal (GI) tract (~5-10 % of total antibiotics) drives resistance evolution in the off-target populations of *Enterococci faecium*, which is a major cause of nosocomial infections.

We have previously shown that the oral administration of cholestyramine (CHA), an ion exchange biomaterial sorbent, prevents DAP treatment from enriching DAP-resistance in populations of *E. faecium* shed from mice. Here, we engineer CHA-DAP interfacial interactions to uncover the antibiotic removal mechanisms from the GI tract. Our findings (https://doi.org/10.1101/2022.06.10.495716) show that the CHA electrostatically adsorbs the anionic antibiotic via a time-dependent diffusion-controlled process. Unsteady-state diffusion-adsorption mass balance describes the dynamics of adsorption well, and the maximum removal capacity is beyond the electric charge stoichiometric ratio because of DAP self-assembly. This study may help design novel biomaterials to remove off-target antibiotics from the GI tract.

Next, we develop an innovative oral adjuvant therapy based on nanocelluloses that removes off-target VAN from the GI tract. The anti-VAN biomaterial comprises a newly emerged class of nanocelluloses, called hairy cellulose nanocrystals (HCNC) and an FDA-approved resin. The high density of HCNC functional groups enables rapid and high-capacity VAN removal while the resin microparticles provide a substrate to immobilize the active nanoparticles. This orally bioavailable biomaterial may limit infections arising from the transmission of antibiotic resistance in VAN-exposed, susceptible individuals.

Extracellular Matrix Stiffness Regulates Histone Modifications During TGFβ1-Induced Epithelial-to-Mesenchymal Transition

Jessica L. Sacco, Ava Self, Elix Sumner, Zachary Vaneman, Stella Kibinda, Chinmay S. Sankhe, Esther W. Gomez

Epithelial cells can acquire a mesenchymal, or stem cell-like, phenotype through a process called epithelial to mesenchymal transition (EMT). EMT is marked by a loss of cell-cell adhesions and downregulation of epithelial genes, such as E-cadherin, as well as a gain in migratory ability and upregulation of mesenchymal genes, such as αSMA. EMT is important in development and wound healing, but if dysregulated, EMT can contribute to fibrosis and cancer metastasis.

Epigenetic reprogramming by histone modifications alters the structure of chromatin to control gene expression. Histone modifications occur during TGFβ1-induced EMT. Extracellular matrix stiffness increases during breast cancer and kidney fibrosis progression and regulates gene expression during EMT. However, it is not clear how matrix stiffness controls histone modifications and histone-modifying enzymes to mediate EMT progression. Here, we examined how mechanical changes in the cellular microenvironment influence histone methylation patterns and gene expression during TGFβ1-induced EMT.

Polyacrylamide (PA) hydrogels were synthesized and tuned to have stiffnesses mimicking healthy mammary tissue (300 Pa) and tumor breast tissue (6300 Pa). Protein levels were monitored using immunofluorescence staining and western blotting. We found that cells cultured on stiff, but not soft, substrata had increased levels of tri-methylation of histone 3 lysine 27 (H3K27Me3) (Figure 1) and increased nuclear levels of the methyltransferase enhancer of zeste homolog 2 (EZH2) in TGFβ1-treated samples. Inhibition of myosin II and ROCK abrogated the TGFβ1-induced increase of H3K27Me3 levels in cells cultured on stiff substrates. Reducing EZH2 activity and expression with a pharmacological inhibitor or siRNA knockdown, respectively, attenuated the TGFβ1-induced increase in H3K27Me3 levels and the expression of EMT markers in cells cultured on stiff substrata. These results indicate that mechanical changes in the cellular microenvironment impact histone modifications and EMT. A better understanding of the signaling pathways implicated in EMT and disease progression may provide targets for therapeutic development.

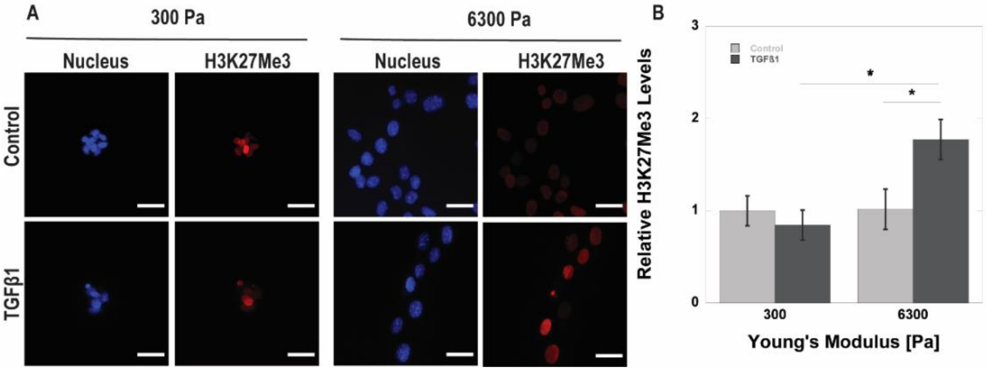

Figure 1. TGFβ1 promotes increased H3K27Me3 levels in NMuMg cells cultured on stiff substrates. (A) Staining for H3K27Me3 (red) and nuclei (blue) in cells cultured on 300 or 6300 Pa substrates and treated with TGFβ1 or a vehicle control. (B) Quantification of relative H3K27Me3 levels. Scale bars = 25 µm; *p<0.05.

Cold Sintering–a New Approach to Reprocess Composite Electrolytes in All-Solid-State Lithium-Ion Batteries

Yi-Chen Lan and Enrique D. Gomez

As all-solid-state lithium-ion batteries (ASSBs) start to dominate the energy-storage device market, studies regarding to recycling spent batteries remain limited and uncomprehensive. During cycling, the formation of secondary phases at electrode-electrolyte interfaces causes the volume change of the battery. The stress evolution may further result in the formation of fractures and eventually the loss of structural integrity in the solid-state electrolyte (SSEs). Despite of the minor decomposition at the interfaces, the majority of bulk SSEs remain active without undergoing significant chemical degradation. To reprocess SSEs, a novel strategy is to repair the fragmented structure avoiding breaking all components into raw materials. Herein, solid-state composite electrolytes, Mg, Sr-doped $Li_7La_3Zr_2O_{12}$ with polypropylene carbonate (PPC) and lithium perchlorate (LLZO–PPC–$LiClO_4$), are reprocessed by cold sintering process. The low sintering temperature allows co-sintering ceramics with polymers and salts, thereby enabling the densification on composite materials. Reprocessed LLZO–PPC–$LiClO_4$ show densified microstructures with ionic conductivities above 10^{-4} S cm^{-1} at room temperature and good long-term stability at 0.1 mA h cm^{-2} over 2000 hours. The reprocessed electrolytes were reassembled into a full cell, $Li_4Ti_5O_{12}$/reprocessed LLZO–PPC–$LiClO_4$/$LiFePO_4$, which demonstrated similar electrochemical properties and capacity retention compared to the pristine cell. This study demonstrates the feasibility of direct reprocessing of SSEs in ASSBs, offering a scalable, low-cost, and sustainable pathway for handling spent batteries at end of life.

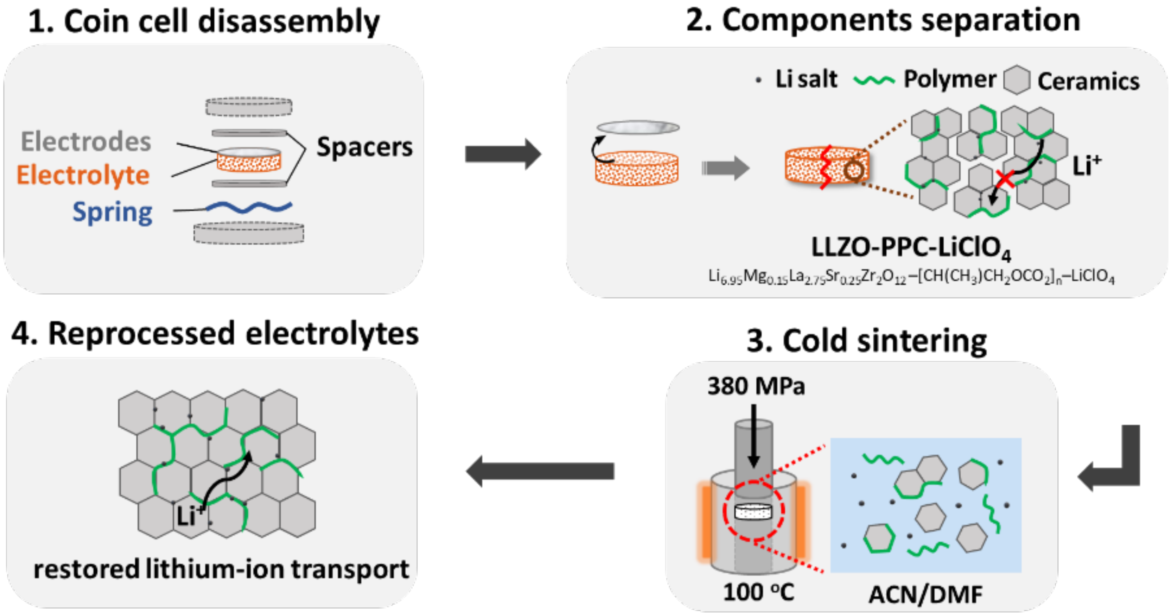

Figure 1. Schematic illustration of reprocessing steps for solid-state composite electrolytes

Understanding the effects of structure of hydrogenated diamond-like carbon on its surface oxidation and frictional behavior in O_2 and H_2O

Seokhoon Jang, Muztoba Rabbani, Prof. Ashlie Martini, and Prof. Seong H. Kim

Hydrogenated diamond-like carbon (HDLC), amorphous carbon (a-C) with a mixture of sp^2- and sp^3-carbon and interstitial or chemically-bound hydrogen (H), has drawn great interest in lubricant applications due to its superlubricity. But its frictional behavior depends on various structural aspects such as sp^2/sp^3 carbon ratio or H content inside the HDLC films, and the superlubricity is often lost in the ambient air upon the oxidation of lubricious HDLC surfaces by O_2 and H_2O. Therefore, one can expect a relationship between HDLC structures and the effects of surface oxidation on its frictional behavior. Deeper understanding of such relationship is prerequisite for advanced solid lubricants to incorporate structural features having tolerance to oxidizing environments for superlubricity in the ambient air. However, studying specifics of the structure dependence of the surface oxidation of HDLC has been limited due to the nature of non-equilibrium structure or a-C; the pristine HDLC is as highly susceptible to oxidizing environments as precious metal catalysts, which provides a complexity of interpretation of the post-testing HDLC surface when its shallow shear plane on the worn HDLC track formed upon frictional sliding gets oxidized by the ambient air during the sample transfer for further chemical analyses. In this study, we investigated two types of HDLC having different endogenous H content inside film: 30- and 40-HDLC (30 and 40 at.% hydrogenated, respectively). Raman analysis displayed that 40-HDLC is more graphitic than 30-HDLC based on the ratio of D-band to G-band and the dispersion rate of G-band, which indicates that 40-HDLC is closer to the thermodynamically favorable structure or graphite and structurally less distorted than 30-HDLC. In Figure 1a, our Langmuir-type kinetics model revealed that 30-HDLC is more susceptible to H_2O- or O_2-oxidation while the model excludes any effects of undesirable air-oxidation, which is consistent with results from ReaxFF-MD simulation. In Figure 1b, the MD simulation showed that the pristine 40-HDLC has more fully coordinated carbon structure and smaller amount of highly reactive carbons than the pristine of less hydrogenated DLC such as 30-HDLC, which is corresponding to the interpretation from Raman. Overall, since more graphitic HDLC showed a lower tribochemical reactivity towards oxidizing gases in atomic and macro-scale, it is conceivable that highly-distorted or strained HDLC structure (or HDLC deviating further from the thermodynamically ideal structure) is more susceptible to tribochemical reaction such as surface oxidation upon frictional sliding.

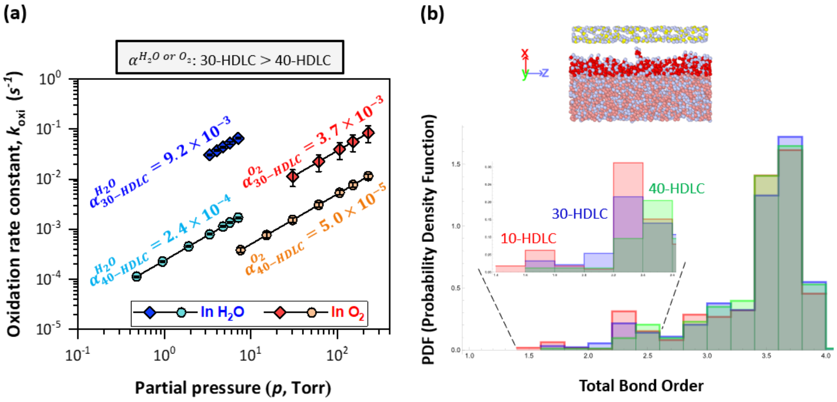

Figure 1. (a) Oxidation rate constant of 30- and 40-HDLC in H_2O and O_2 gas environments estimated by our Langmuir-type kinetics model and (b) histogram of total bond order of the pristine 30- and 40-HDLC before any surface reactions obtained by the ReaxFF-MD simulation.

Session 1: Room B

Structural inhomogeneity of cellulose assembly in plant cell wall affecting anisotropic mechanical property

Jongcheol Lee[1], Juseok Choi[1], Luyi Feng[2], Jingyi Yu[3], Yunzhen Zheng[3], Qian Zhang[3], Yen-Ting Lin[1], Saroj Sah[3], Ying Gu[3], Sulin Zhang[2], Daniel J. Cosgrove[3], and Seong H. Kim[1]*

Cellulose microfibrils (CMFs) in plant cell walls are a major load-bearing component in plant primary cell walls, and their orientation is known to be a key factor to determine the mechanical properties of the cell wall. Plant epidermis has been widely used as a model system for the primary cell wall to study the cellulose structure and tissue mechanics because of its ease of access for characterization. However, the structural information of CMFs in epidermal walls has often been interpreted assuming that the whole tissue has a uniform structure. Here, we report distinct CMF assembly patterns in the flat face region of the epidermal cell and the edge region of the cell where two cells meet. The vibrational sum frequency generation (SFG) imaging analysis found that the CMF orientation in the cell edges is preferentially aligned perpendicular to the anticlinal plane. This discovery explains the previously observed anisotropic mechanical properties of single epidermal cell wall tissues and resolves discrepancies in microfibril structure obtained with different techniques.

---

[1] Department of Chemical Engineering, Materials Research Institute, Pennsylvania State University, University Park, Pennsylvania 16802, USA.
[2] Department of Engineering Science and Mechanics and Bioengineering, Materials Research Institute, Pennsylvania State University, University Park, Pennsylvania 16802, USA.
[3] Department of Biology, Pennsylvania State University, University Park, Pennsylvania 16802, USA.

Depth filters for removal of HCP during monoclonal antibody production

Liang-Kai Chu, Dr. Ehsan Allah Espah Borujeni, Dr. Xuankuo Xu, Dr. Andrew L. Zydney

The production of recombinant proteins involves growing mammalian cells in large bioreactors. Over the past 30 years, the volumetric yield for monoclonal antibody process has increased more than 20-fold with a maximum cell density above 20 million cells/mL. The high amount of biomass poses a great challenge in downstream clarification not only because of filter fouling resulting from insoluble cell debris but also from the added burden on expensive chromatography steps due to the high levels of host cell proteins (HCP) that must be removed by the downstream process.

Depth filters are widely used in downstream processing for recombinant protein manufacturing. Depth filters can provide primary clarification to remove cells, cell debris, and other large impurities, or they can provide additional clarification / purification in combination with other unit operations. Depth filters use a combination of size exclusion and adsorption (due to both hydrophobic and electrostatic interactions). The objective of this project was to develop a fundamental understanding of the factors controlling HCP removal by a set of Millipore Millistak+ µPod series depth filters with different pore size and chemistry. Data were obtained with a series of model proteins that span the charge and hydrophobicity of typical HCP.

Typical breakthrough curves for several proteins are shown in Figure 1. In each case the binding capacity was evaluated by integration of the breakthrough curve. A Langmuir isotherm was then fit to the binding capacity data as a function of the protein concentration with typical isotherm profiles shown in Figure 2. Data for the X0SP depth filter containing a synthetic silica filter aid show high binding of positively-charged proteins like α-chymotrypsin, suggesting the importance of electrostatic interactions on HCP removal. In contrast, data obtained with depth filters containing diatomaceous earth suggest that hydrophobic interactions play an important role in protein binding. These results provide new insights into the role of depth filter and protein chemistry on HCP removal in bioprocessing.

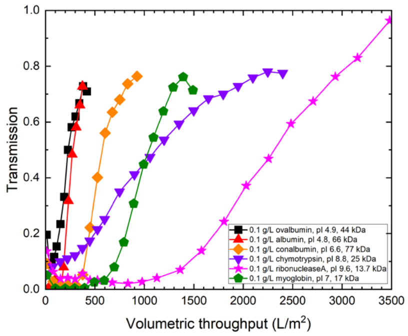

Figure 1. Breakthrough curves for positively-charged ribonuclease A (13.7 kDa) and α-chymotrypsin (25 kDa) filtered through X0SP filter show much greater binding than seen with the neutral and negatively-charged proteins.

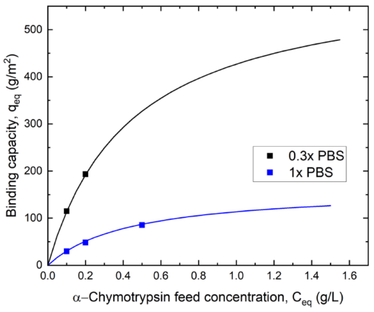

Figure 2. Both negatively charged albumin (not shown) and positively charged α-chymotrypsin bind much less in high ionic strength buffer than they do in 0.3x PBS buffer when filtered through X0SP. The results suggest that electrostatic interactions are one of the key mechanisms governing capture of the model proteins in these depth filters.

Investigation of the mesoscale structural assembly of cellulose microfibrils in plant cell walls using sum-frequency generation vibrational spectroscopy

Juseok Choi, Jongcheol Lee, Mohamadamin Makarem, Shixin Huang, and Seong H. Kim*

Mesoscale structural assemblies of cellulose microfibrils (CMFs) play a key role in the mechanical properties of plant cell walls. However, due to the structural complexity of plant cell walls which are a mixture of polymeric components, it is challenging to characterize CMF structures. Sum-frequency generation (SFG) spectroscopy is a unique technique to detect crystalline structures even interspersed in amorphous domains because non-centrosymmetric arrangement of vibrational modes is required to generate SFG signals. Because cellulose is the only crystalline component among the major cell wall materials, SFG technique can be used for cellulose studies without the interference of other amorphous cell wall components.

However, it is hard to interpret SFG signals to understand the structure of CMFs in plant cell walls because SFG signals can be affected by a lot of parameters of laser geometry as well as the natural properties of vibration modes of celluloses. In order to overcome the difficulties of SFG interpretation, understanding SFG theories especially about how signals change as vibration mode arrangements and the development of simulation tools based on theoretical approaches are needed.

In this proposal, a numerical simulation method will be described to predict SFG signals of CMFs in plant cell walls. This simulation method will cover the orientation of CMFs as well as their assemblies in 3-D amorphous domains with specific parameters (e.g., CMF diameters, the distance between CMFs, and directional excess) to calculate SFG intensity. For the verification of this simulation algorithm, two examples were used: the symmetric and asymmetric stretch modes of the CH_3 and CH_2 groups of ethanol at 2D air/liquid interface and a thin film of uniaxially-aligned cellulose nanocrystals. And with the newly developed numerical simulation tool, it can also be applied to any SFG-active nanodomains interspersed in three-dimensional amorphous matrices.

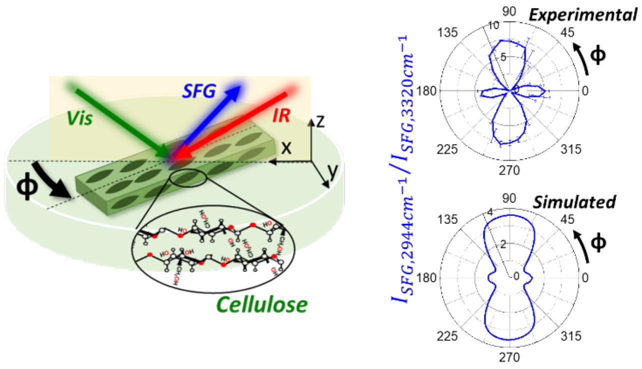

Figure 1. Azimuth angle polar plot of experimental or numerically simulated 2944/3320 cm^{-1} SFG intensity ratio of cellulose nanocrystal thin film

A fundamental model to describe asymmetric ion transport in bipolar membranes

Harrison J. Cassady, Dr. Michael A. Hickner

Ion exchange membranes are a class of dense membranes made from charged, hydrophilic polymers. Ion exchange membranes are typically grouped into two categories based on the sign of the charge they select for: anion exchange membranes (AEM) select anions and reject cations, while cation exchange membranes (CEM) select cations and reject anions. By laminating an AEM with a CEM, a composite membrane called a bipolar membrane (BPM) is created.

BPMs reject the transport of salts across them, but allow the passage of an ionic current by the creation of water at the BPM junction interface. This unique property provides wide-reaching applications for BPMs, including but not limited to desalination, mineral extraction, energy storage and conversion (in both redox flow batteries and fuel cells), and as circuit elements for electrochemical circuits.

This work presents a model for describing the non-ideal case of ion transport across a BPM under a diffusional driving force. The model is derived using fundamental mass transport equations, and is used to explain observed asymmetry of ion transport across a BPM as a function of specific membrane parameters.

Session 2: Room A

Stable All-Solid-State Sodium-Sulfur Batteries Enabled by Sodium-Antimony Alloy Anode and Confined Sulfur Cathode

Li-Ji Jhang[1], Daiwei Wang[2], Alexander Silver[3], Xiaolin Li[4], David Reed[4], Donghai Wang[2]

[1]Department of Chemical Engineering, The Pennsylvania State University, University Park, Pennsylvania 16802, United States, [2]Department of Mechanical Engineering, The Pennsylvania State University, University Park, Pennsylvania 16802, United States, [3]Department of Materials Science and Engineering, The Pennsylvania State University, University Park, Pennsylvania 16802, United States, [4]Energy and Environment Directorate, Pacific Northwest National Laboratory, Richland, Washington 99354, United States

All-solid-state sodium-sulfur (Na-S) batteries are promising for stationary energy storage devices because of their low operating temperatures (less than 100 °C), improved safety, and low-cost fabrication. Using Na alloy instead of Na metal as an anode in Na-S batteries can prevent dendrite growth and improve interfacial stability between the anode and solid electrolytes to achieve long-cycling stability. A high-sulfur content cathode possessing high sulfur utilization is also important to enable an energy-dense Na-S battery. In this work, we studied Na-Sb and Na-Sn alloy anodes and demonstrated the superiority of Na_3Sb alloy undergoing a stable Na alloying/dealloying process at 0.04 mA cm^{-2} for over 500 hours. Combining the optimized Na_3Sb alloy anode with sulfur-carbon composites prepared by the vapor deposition approach, the full cell shows a high sulfur specific capacity and improved rate performance. Moreover, the all-solid-state Na alloy-S battery can deliver a high initial discharge specific capacity of 1377 mAh g^{-1} and maintain good capacity retention of 70% after 180 cycles at 60 °C. Post-cycle characterizations show that both the anode and cathode perform a reversible discharge/charge process after the 1st cycle, and the cathode undergoes significantly rearranged distributions of carbon and solid-state electrolytes after 180 cycles due to severe volume change induced by repeated sodiation/desodiation process.

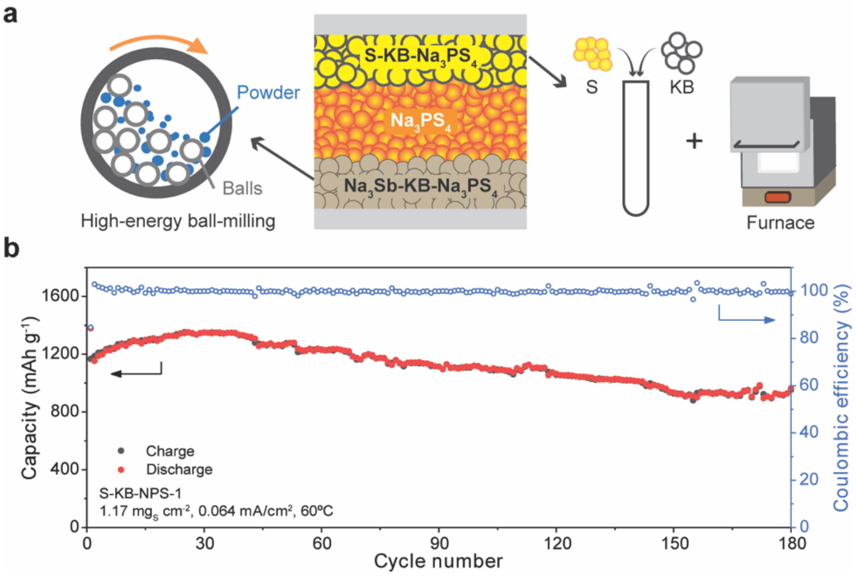

Figure 1. (a) Schematic configuration and fabrication of a Na alloy-S battery. (b) Long-term cycling performance of a Na alloy-S battery under 0.064 mA cm^{-2} at 60 °C.

Catalytic Co-Pyrolysis of Polyolefins and Polyethylene Terephthalate (PET) with Zeolite Catalysts

Sean Timothy Okonsky, Dr. J. V. Jayarama Krishna, Dr. Hilal Ezgi Toraman

Pyrolysis, a process which heats feedstocks in the absence of air, can be used to convert plastic waste into valuable fuels and chemicals. The addition of zeolite catalysts into the pyrolysis process can decrease the temperature needed for polymer degradation and can help to modify the product distribution. While the catalytic pyrolysis of polyolefins such as low-density polyethylene (LDPE) and polypropylene (PP) is well researched, the catalytic pyrolysis of PET is not researched as much due to the oxygen present in PET’s structure which causes a high amount of catalyst coking. Polyolefins and PET can inherently be mixed in unsorted plastic waste as well as in multilayer packaging. Researching the interactions between polyolefins and PET during catalytic pyrolysis can provide insight on how PET can be included with polyolefins as a pyrolysis feedstock without sacrificing product quality. Thermogravimetric analysis (TGA) experiments revealed interactions during the catalytic co-pyrolysis of LDPE and PET with three zeolite catalysts (HZSM-5, H-Beta, HY). Lumped model-fitting kinetics were used to derive kinetic parameters for a reaction scheme which was able to capture these interaction effects. Quantifying catalyst deactivation via pyridine temperature programmed desorption (Pyr-TPD) and deriving initial guess values for kinetic parameters via isoconversional approach has been used as a way to improve the kinetic modelling. Micro-pyrolysis gas chromatography mass spectrometry (Py-GC/MS) experiments revealed HY catalyst resulted in higher synergy% (142%) than HZSM-5 (3%) for alkylated benzenes during the catalytic co-pyrolysis of LDPE and PET, based off a semi-quantitative approach from GC/MS area% values. Coupling a micro-pyrolysis reactor with a two-dimensional gas chromatography system with a time-of-flight mass spectrometer and a flame ionization detector has been used for enhanced separation and quantification capabilities to gain further insight on the interactions occurring during the catalytic co-pyrolysis of polyolefins and PET with zeolite catalysts.

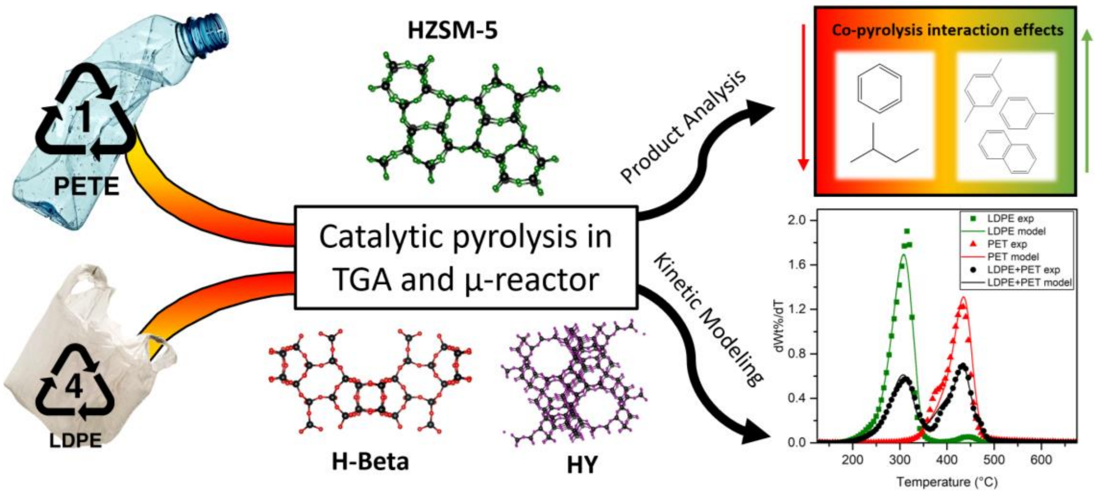

Designing retro-biosynthesis pathways to chemical products: Algorithmic improvements and applications

Vikas Upadhyay, Dr. Costas D. Maranas

Retro-biosynthetic approaches have made significant advances in predicting synthesis routes of target biofuel and bio-renewable design to the biodegradation or funneling complex aromatics and chemicals with industrial interest. It is also a multi-disciplinary task that requires knowledge and encoding of the relevant biochemistries, biophysical understanding of enzymatic activity and specificity, understanding the thermodynamic feasibility of individual enzymatic steps, and subsequent host selection and metabolic engineering. Next, the use of only cataloged enzymatic activities limits the discovery of new production routes. The retro-biosynthetic algorithms increasingly use novel conversions that require altering an existing enzyme's substrate or cofactor specificity to complete the pathway. However, identifying and re-engineering enzymes for novel conversions needed to complete the pathway are currently the bottlenecks in implementing these designs. Therefore, we focus on designing computational tools that can ensure de novo pathway design requirements within a single framework. Hence, we designed dGPredictor, and EnzRank, which can be integrated within our pathway design tool novoStoic to aid relevant tasks. dGPredictor predicts the Gibbs energy change for biochemical reactions and reactions involving novel structures, which can be used to ensure the thermodynamic feasibility of pathways. The integration within novoStoic prohibits reaction steps for which the directionalities are thermodynamically infeasible. EnzRank is a convolutional neural network (CNN) based approach to select enzyme candidates for novel conversions in the pathway design. EnzRank rank-order existing enzymes in terms of their suitability to undergo successful protein engineering through directed evolution or *de novo* design towards the desired specific substrate activity. Thus, EnzRank can help novoStoic find enzyme candidates for a novel reaction in biosynthesis pathways. Hence, this work aims to build a unified web-based interface that takes a target chemical as input and designs de novo pathways for its synthesis, ensuring thermodynamic feasibility and selecting enzymes for the novel reaction steps with designed pathways.

Electricity generation from hydraulic fracturing wastewater using a reverse electrodialysis stack

Arash Emdadi[1], Jamie Hestekin[2], Lauren F. Greenlee[1], Bruce Logan[1,3]

[1]Chemical Engineering Department, Pennsylvania State University, University Park, PA

[2]Chemical Engineering Department, University of Arkansas, Fayetteville, AR

[3]Civil and Environmental Engineering Department, Pennsylvania State University, University Park, PA

Hydraulic fracturing (HF) wastewater is produced during the hydraulic fracturing process where crude oil and natural gas are produced. The technology uses a diluted solution (water) including different additives. HF wastewater, which is produced during the process, is a very concentrated solution including different ions, and organic compounds. As an environmental challenge, HF wastewater has harmful effects on the soil, air, and water resources. In this study, a reverse electrodialysis stack is employed to produce electricity from the salinity gradients between the feed solution and produced HF wastewater. A reverse electrodialysis (RED) system is consists of selective ion exchange membranes (IEMs) know as, cation exchange membranes (CEMs) and anion exchange membranes (AEMs). The AEMs are selective to anions; however, the CEMs allow cations to pass. Due to concentrations gradient, cations and anions will diffuse toward cathode, and anode respectively. Because of redox reactions on the surface of electrodes (titanium (Ti) coated with iridium (Ir), and ruthenium (Ru)), the electricity can be produced. In this study, a RED stack including 10 cell pairs was built, and a real sample of HF wastewater was employed. Based on the results, a gross power density around 3.6 $\frac{W}{cp.m^2}$ achieved. IEMs characterizations including permselectivity, and electrical resistance were investigated for both CEMs and AEMs in the presence of HF wastewater, and other artificial salt solutions. Based on the results, presence of divalent ions reduces the permselectivty of CEMs, and IEMs. However, the high concentration of HF wastewater reduces the ohmic resistance of the stack and increases the gross power density of RED stack. Results of this study indicate that HF wastewater can be considered as a promising source of electricity generation to reduce the environmental impacts of HF process.

Session 2: Room B

Rational Engineering of Explosive-sensing Soil Bacteria

Erin Essington, Dr. Daniel Cetnar, Emily Gradinette, Dr. Terrance Bell, Dr. Howard Salis

Buried explosives, whether left over from past conflicts or recently buried by enemy combatants, pose a serious threat to both civilians and warfighters. Sites containing buried ordnance have soil with elevated levels of 2,4-dinitrotoluene (DNT) and 2,4,6-trinitrotoluene (TNT). We have engineered genetic circuits inside soil bacteria (*Bacillus subtilis*) detect trace amounts of DNT/TNT and respond by producing an odorant (IBMP, 2-methoxy-3-isobutylpyrazine) that is readily detectable by humans and canines from stand-off distances. To do this, we designed and constructed over 80 genetic circuits and integrated them into the *Bacillus subtilis* genome, utilizing DNT/TNT-sensing promoters, DNT/TNT-sensing riboswitches, DNA-flipping integrases, and an IBMP-producing enzyme. We optimized genetic circuit function by rationally tuning genetic part function, including ribosome binding sites to control translation rate and anti-sense promoters to reduce transcriptional leakiness, identifying 8 robust genetic circuit variants that reliably sense and respond to TNT. We also measured the growth and persistence of engineered *Bacillus subtilis* strains in wild soil, confirming that growth continued, and functionality persisted for at least 4 weeks. These genetically engineered in-soil sense-and-respond bacteria provide a new countermine capability and a platform for detecting specific metabolites inside soil systems.

Using machine learning approaches to estimate enzyme kinetic parameters

Veda Sheersh Boorla[1], Costas D. Maranas[1*]

[1] *Department of Chemical Engineering, The Pennsylvania State University, University Park, PA 16802, USA*

Abstract

The catalytic turnover number (k_{cat}) is a key kinetic property an enzyme defined as the maximal number of molecules of substrates converted to products per active site per unit time. Accurate and generalizable methods for estimating enzyme kinetic parameters such as the one presented here can be invaluable for applications ranging from metabolic modeling to enzyme re-engineering. Enzyme databases such as BRENDA[1] contain a repository of turnover numbers measured *in vitro.* However, the available data is noisy due to various experimental conditions and lack of proper annotations for several entries. We curated a dataset of ~6,000 turnover numbers from BRENDA by applying several quality filters. Using this dataset, we trained a convolutional neural network (CNN) model to learn amino-acid embeddings that accurately estimate k_{cat} values when used as enzyme features along with morgan fingerprints as substrate features. The trained model achieved an average Pearson correlation coefficient of 0.78 (standard deviation 0.008) and an average root mean squared error of 0.96 (standard deviation 0.061) in a 5-fold cross validation evaluation. The root mean squared error of 0.96 in log scale corresponds to less than an order of magnitude error in linear scale which is quite low compared to the overall range of k_{cat} values (1E-06 to 1E+07). The low standard deviations across cross-validation suggests a robust and generalizable training across the entire dataset. The success of our model can be attributed to the ability of CNNs to extract complex local patterns of amino acid residues that may be responsible for actual enzyme-substrate interactions on the molecular level. Comparison of our model to existing methods along with its current limitations and provision for improvements will be discussed. In particular, the use of state-of-the-art protein language model embeddings as features and the use of graph-based architectures that overcome the limitations and CNNs and provide more meaningful insights will be discussed. By training ML models to accurately capture the mapping between amino acid mutations and changes in turnover numbers, they can be used to guide directed evolution and/or targeted enzyme engineering approaches.

References:

1. Chang, Antje et al. “BRENDA, the ELIXIR core data resource in 2021: new developments and updates.” Nucleic acids research vol. 49,D1 (2021): D498-D508.

Analysis of Ribosome Regulators in the Formation and Resuscitation of Persister cells

Joy Muthami, Dr. Thomas Wood

There is urgent need to address multidrug tolerant bacteria because bacterial infections are responsible for 17 million+ infections yearly. Three ways bacteria often resist antibiotics are by becoming, **(i)** resistant, through mutation, **(ii)** tolerant, due to slow growth, or **(iii)** persistent, metabolically dormant cells, without undergoing any mutations. Since persister cells combat antibiotic treatment by sleeping through it, once the antibiotic is removed, they awake and reconstitute infection, which may be the cause of many recurring infections (e.g., tuberculosis, cystic fibrosis, and Lyme disease). The mechanism for persister cell formation and resusitation is not fully known. Recently it has been shown that persister cells form and resuscitate by inactivating and activating ribosomes respectively using the intercellular signals guanosine (penta)tetraphosphate ((p)ppGpp) and cyclic adenosine monophosphate (cAMP). In *Escherichia coli* inactivation is mediated by the ribosome associated inhibitor (RaiA), ribosome modulation factor (Rmf), and hibernation promotion factor (Hpf), while activation is medicated by the ribosome resuscitation factor (HflX). With the aim to validate our ppGpp ribosome dimerization persister (PRDP) model, we assay transcription of *raiA, rmf, hpf,* and *hflX* genes for cells entering the persister state and for resuscitating cells. We show that persister formation and resuscitation might not be caused by induction and repression of *raiA, rmf, hpf,* and *hflX* genes but rather the inactivation and activation of RaiA, Rmf, Hpf and HflX proteins.

Kinetic asymmetry determines the direction of enzyme chemotaxis

Abstract:

Enzyme chemotaxis is the directional motion of enzyme molecules towards or away from a gradient of their respective substrates and products. The phenomenon has wide ranging implications for not just the modern-day applications, such as drug delivery and disease detection, but also for determining the physiochemical driving force behind origin of life and its subsequent evolution. While there have been several hypotheses on why enzymes chemotax, the underlying principle remains to be fully elucidated. In this study, we propose a mechanism of chemotaxis based solely on the diffusion and chemical kinetics of the enzyme molecules. We show two factors. 1) kinetic asymmetry, the difference between the unbinding rates of the substrates and the products and 2) diffusion asymmetry, the difference in the diffusivities of the unbound and the bound form of the enzyme, govern the direction of enzyme chemotaxis. Our model captures the non-equilibrium distribution of enzyme molecules while they maintain complete mechanical equilibrium with the surroundings and thus fulfills the criterion of low Reynold’s number regime.

We begin our analysis with a uniform concentration of an enzyme and a constant gradient of substrate and product in the domain. We use trajectory thermodynamics to determine the role of kinetic and diffusion asymmetry in determining the direction of enzyme chemotaxis. We confirm the role of kinetic asymmetry by solving rate equations for the enzyme and obtaining the steady state enzyme distribution. Furthermore, it has been suggested in literature that in evolution of simple matter into complex life-like structures, the most favored state is the one that has the maximum rate of energy dissipation. Our work is important in this context, as we have been able to show that the rate of dissipation plays no role in determining the direction of chemotaxis. Thus, we conclude that kinetic and diffusion asymmetry constitute the key driving forces behind enzyme chemotaxis and further suggest may play a role in the evolution of simple matter into complex systems.

Authors:

Niladri Sekhar Mandal[a], Ayusman Sen[a,b], R. Dean Astumian[c*]

[a]Department of Chemical Engineering, The Pennsylvania State University, University Park, PA 16802
[b]Department of Chemistry, The Pennsylvania State University, University Park, PA 16802
[c]Department of Physics and Astronomy, [c]University of Maine, Orono, Maine 04469

Session 3

Block copolymer templated extended surface PGM nanostructures as model electrocatalysts

Deepra Bhattacharya and Christopher Arges*

Templating platinum group metal (PGM) nanostructures from microphase separated block copolymer (BCP) thin films allows for electrocatalytic activity to be studied on highly ordered model surfaces with tuneable feature size and morphology, thereby enabling the kinetics of electrocatalytic reactions to be probed as a function of nanoscale geometry. This talk will discuss recent endeavors in the Arges research group to establish fundamental relationships between electrocatalyst functional response, nanoscale geometry, and fabrication pathways via systematic investigation using BCP templated PGM nanostructures. PGM electrocatalysts were prepared from liquid phase (wetness impregnation) and gas phase (e-beam evaporation, magnetron sputtering, atomic layer deposition) fabrication pathways and tested on both two-electrode interdigitated electrode (IDE) chips and three-electrode rotating disk setups for model electrochemical reactions such as Hydrogen evolution/oxidation (HER/HOR) and oxygen reduction (ORR) using both liquid and solid electrolytes. The electrocatalyst nanostructures were characterized via a combination of electron microscopy, X-ray diffraction, X-ray photoelectron spectroscopy, and grazing incidence small angle X-ray scattering (GISAXS). Pt content of the catalysts were determined via microwave leaching and digestion of the electrocatalyst thin films followed by Inductively Coupled Plasma Mass Spectroscopy (ICP-MS). The talk will also showcase the use of the electrocatalysts fabricated on interdigitated electrode chips for high throughput comparative performance evaluation of high temperature proton exchange membranes (HT-PEMs) for applications in fuel cells and electrochemical hydrogen pumps.

Heterogeneous Catalysis with Photocatalytic Polymer Brushes on Glass Beads

Sarah Freeburne, Kirsten Bell, Dr. Christian W. Pester

Photocatalysis provides many benefits in comparison to thermal catalysis. These benefits include the ability to perform reactions under mild conditions, such as at ambient temperatures and pressures. Light sources may be inexpensive or high-powered, examples include LED lights, lasers, or even the sun. Heterogeneous catalysis occurs when the phase of the catalyst is different than the phase of the reaction. This is beneficial because it can simplify separation procedures to remove catalysts from the reaction mixture. Examples for heterogeneous photocatalysts include nanoparticles, metal oxide surfaces, or polymer networks. This work employs a solid catalyst mixed in solution with reactants in the liquid phase and uses polymer brushes – i.e., polymers tethered covalently to a glass surface – as the heterogeneous photocatalyst. An important feature of this system is that the glass bead supports are much larger than typical supports (e.g., nanoparticles with grafted photocatalysts). This facilitates catalyst recovery and recycling. Since the catalytic polymer brushes remain covalently attached to the glass bead surfaces, catalyst recovery may be accomplished with simple filtration. This presentation demonstrates the efficacy of photocatalytic polymer brush-functionalized glass beads supports in photocatalytic radical dehalogenations, cyclic condensations, and polymerization reactions. This platform may be further expanded to include different photocatalysts, as well as different supports to expand the photocatalytic platform.

Incorporating electrode-electrolyte interfacial effects on the specific adsorption of alkali cations on late transition metal surfaces using DFT methods

Andrew Jark-Wah Wong, Bolton H. Tran, Naveen Agrawal, Scott T. Milner, and Michael J. Janik

Cations within the electrolyte have pronounced effects on the kinetics and selectivity of relevant electrocatalytic reactions in batteries, fuel cells, electrolysis cells, and carbon capture technologies. Particularly, specific adsorption of cations can competitively adsorb to active sites and interact strongly with the interfacial electric field, altering the interfacial structure of the electrochemical double layer (EDL). Incorporating the effects of the local electric field and interfacial solvation during specific cation adsorption is important in the development of electrocatalysts to better understand how cations can tune the overall activity of electrocatalytic reactions. However, modeling the EDL structure and distribution of ions is not trivial due to the complexities within the interface. Our group has developed a compartmentalized DFT Helmholtz approach to model elementary electrocatalytic reaction energies and barriers while deconstructing the complexities of the EDL. We extend this approach to investigate the potential dependence of specific cation adsorption equilibrium on late transition metal surfaces. In this study, we used DFT methods to quantify the specific interactions between (hydrated) alkali cations and the electrode, and between cations and specific solvent molecules. We then investigated the sensitivity of modeling choices of solvation and electrification towards the equilibrium of specifically adsorbed cations. We found that the potentials where cations specifically adsorb on late transition metal surfaces can vary by over 1 V-NHE depending on the approach used to model the effects of solvation within the EDL (explicit H_2O molecules, implicit solvation, or FF-MD description). Cations are sensitive to the local field effects within the EDL, specifically the modeling choices of the effective dielectric constant (ε) and width (d) of the EDL. We will discuss how the atomistic description of Force-Field Molecular Dynamics (FF-MD) simulations can assist in modeling specific cation adsorption by incorporating extended ion-solvent and ion-electrified interactions within the EDL, which can better inform our DFT Helmholtz model.

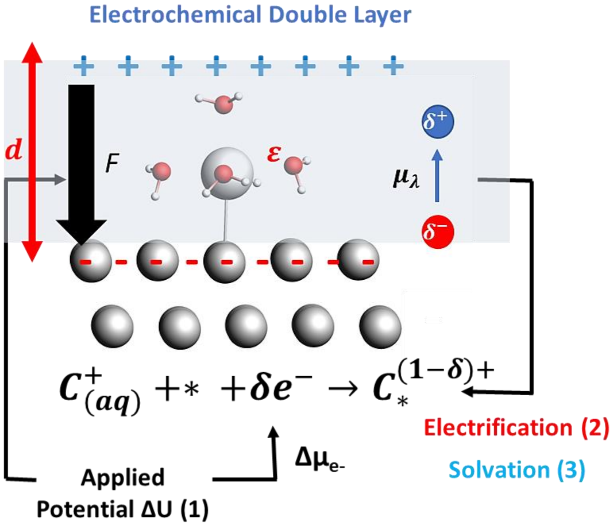

Figure 1: Overview of the DFT Helmholtz approach to model specific cation adsorption within the EDL.

Computational Evaluation of Selective Hydrogenation Reactions on TiO_2-supported Single Atom Catalysts

Jeremy Hu, Michael J. Janik, and Konstantinos Alexopoulos

Single atom catalysts have caught recent interest due to their improved selectivity and activity otherwise unseen in their traditional heterogeneous catalyst counterparts. Experimentally, single atom catalysts dramatically improve selectivity in hydrogenation reactions of complex carboxylic acids derived from bio-mass or plastic waste. Even metals traditionally dismissed as poor hydrogenation catalysts, such as Ag, can be active for hydrogen activation and spillover when deposited as single atoms on anatase TiO_2. However, many questions remain unanswered about how the structure and redox behavior of the extended TiO_2 support affect the elementary reactions (e.g., C-H or O-H bond formation) that may favor one hydrogenation product over another.

In our work, we provide fundamental insight using computational tools such as density functional theory (DFT) on the selective hydrogenation of benzoic acid, a carboxylic acid derived from plastic waste. We use DFT to examine reaction energies of various reaction pathways to gauge how the catalyst structure affects the formation of different hydrogenation products. Additionally, we study how the redox behavior of the support and spillover H atoms can differentially stabilize intermediate reaction species that aid in the selective formation of hydrogenation products.

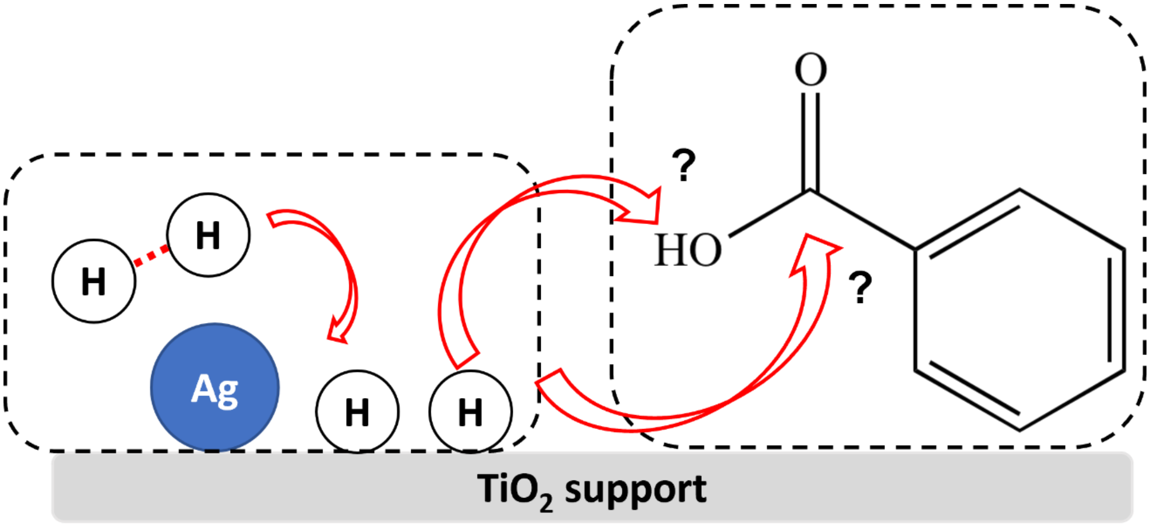

Enhanced Electrochemical Phosphate Recovery from Wastewater: Implications of Pulsating Anode Potential

Ruhi Sultana, Mike Janik, and Lauren Greenlee

Phosphorus (P) is essential for life and is used in fertilizer to sustain global food production. Approximately 95% of the P mined worldwide from non-renewable phosphate rock reserves is used as fertilizer. However, phosphate production is expected to peak as early as 2030, and post-peak, phosphate production, and therefore food supply, will be restricted by dwindling resources, strained economics, and reduced rock quality, with remaining resources expected to last 50-300 years. The limited supply of phosphate demands P conservation by changing the food production system, from fertilization to wastewater treatment. Stuvite ($MgNH_4PO_4*6H_2O$) has been recognized as a high-value, slow-release, effective fertilizer that can be obtained from both solid (e.g., food, animal, and human waste) and liquid wastes (e.g., wastewater from industrial, municipal, and agricultural operations). The goal of our research is to recover struvite from wastewater using an alkaline electrochemical reactor with a magnesium alloy anode and a cathode constructed of standard catalysts for reducing water to hydrogen gas and hydroxide.

The primary mechanism for magnesium corrosion is localized, where shallow, irregular pits form and spread across the metal surface. Once Mg^{2+} is in solution, metal salt (i.e., $Mg(OH)_2$ and $MgCO_3$) precipitation and electrode surface fouling occurs, resulting in increased energy demand and reduced struvite recovery. In contrast, a novel pulsating (or dynamic) voltage approach using sinusoidal waveforms induces "fatigue" rupture of the passivation layer and accelerates Mg^{2+} release, which enhances struvite precipitation. Mg^{2+} release significantly increases by ~120% relative to constant voltage applications, which results in ~2x higher phosphate recovery. Analysis by X-ray diffraction (XRD) and scanning electron microscopy (SEM) indicates that the precipitate contains struvite. Inductively coupled plasma mass spectrometry (LA-ICP-MS) is also used to characterize electrode surfaces in the presence of dynamic voltages and confirms greater breakdown of surface film thickness. Our experimental findings on how pulsating voltage can be coupled with electrochemical processes designed to recover precipitates are a novel contribution to electrochemistry research that will have a significant impact on wastewater treatment, nutrient management, and circular economy electrochemical technologies. Concurrent development of a first-of-its-kind bench-scale Mg bead filled packed bed electrochemical reactor demonstrates the technology concept and allows for preliminary optimization and engineering design of the electrochemical cell. Overall, our research has provided a better understanding of the necessary framework, as well as the associated challenges and benefits, for P recovery via wastewater-produced struvite fertilizer.